Miniemulsion Polymerization Monitoring Using Off-Line Raman Spectroscopy and In-Line NIR Spectroscopy

Paula Maria Nogueira Ambrogi, Maria Magdalena Espinola Colmán, Reinaldo Giudici*

Miniemulsion polymerization has been extensively studied in the last decade due to its advantages when compared with conventional emulsion polymerization. In this work, monomer conversion and particle size are monitored during miniemulsion polymerization of styrene using in-line near-infrared (NIR) spectroscopy and at-line Raman spectroscopy. Gravimetric analysis and dynamic light scattering have been used as off-line reference measurements. Good agreement has been found between off-line data and the values predicted by NIR and Raman spectroscopy for conversion. The values of average particle size are well predicted from the NIR spectra with the respective calibration model, but the predictions from Raman spectra present some slight discrepancies for particle size. The results show a decrease of the average particle size during the initial period of the polymerization, indicating the occurrence of nucleation mechanisms other than the classical droplet nucleation. These results indicate that insightful information can be obtained by monitoring miniemulsion polymerizations with the use of spectroscopic techniques.

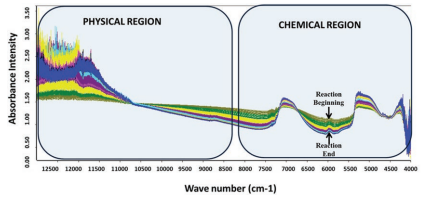

1. Introduction

The heterogeneous nature of the miniemulsion polymerization process involves the use of a smaller amount of organic solvent when compared with bulk and solution polymerization, making it more environmentally friendly. Moreover, the apparent viscosity of the reactor content in heterogeneous polymerization process is lower, thus providing a better heat transfer when used in industrial plants where heat exchange is usually a process limitation. In addition, the environmental laws are more concerned about polymers based on organic solvents and there is a tendency to substitute solvent-based polymers by water-borne latex, increasing the importance of conventional emulsion and miniemulsion polymerization.

In comparison with conventional emulsion polymerization processes, miniemulsion polymerization presents clear advantages because polymerization takes place inside the monomer droplets, which allows using monomers and other highly hydrophobic components in the formulation. Therefore, these components do not need to diffuse in the aqueous medium as in emulsion polymerization.[1–4]

The miniemulsion polymerization process starts with the preparation of the monomer miniemulsion and, after that, the addition of an initiator starts the polymerization. A standard miniemulsion formulation uses water as continuous phase, monomer as disperse phase, surfactant to stabilize the particles droplets, costabilizer to avoid diffusional degradation (Oswald Ripening), and buffer to stabilize the pH of the medium.[5] Constant particle size, use of costabilizers, use of surfactant below the critical micellar concentration, and inexistence of mass transport through the aqueous phase are

Dr. P. M. N. Ambrogi, Dr. M. M. E. Colmán, Prof. R. Giudici
Universidade de São Paulo
Escola Politécnica
Department of Chemical Engineering
Av. Prof. Luciano Gualbertvo
travessa 3, No. 380, 05508-010 São Paulo, SP, Brazil
E-mail: rgiudici@usp.br

DOI: 10.1002/mren.201600013

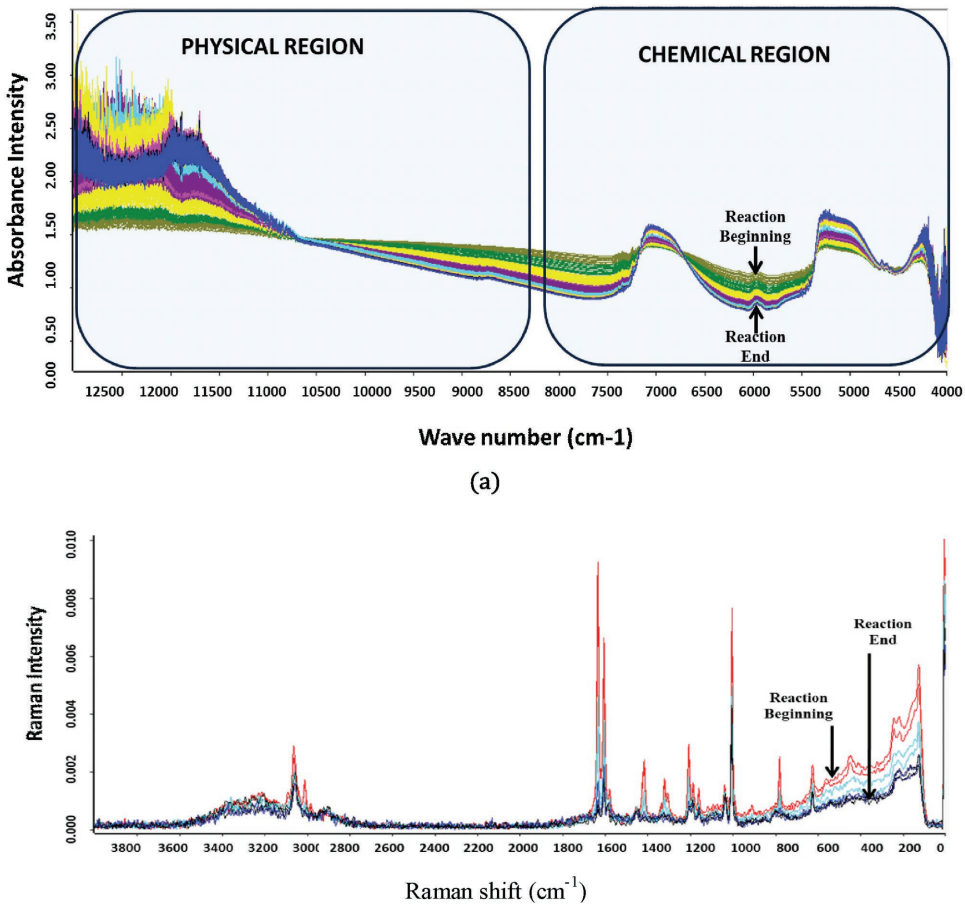

Figure 1. a) NIR spectra changes during miniemulsion polymerization, indicating the spectral region with chemical information and the spectral region with physical information; b) Raman spectra changes during miniemulsion polymerization (horizontal axis: Raman shift, vertical axis: Raman intensity).[25]

the most important characteristics of the miniemulsion polymerization.[6]

Ideally, miniemulsion polymerization would be dominated by droplet nucleation, so that each initial monomer droplet would be converted into a polymer particle. However, some works have reported that the final polymer particle size distribution may significantly differ from the initial size distribution of the monomer droplets, with ratios Dg/Dp (between the initial average droplet size and final average polymer particle size) lower than 1. This is clear evidence that other nucleation mechanisms are taking place. Similar results have been reported in the literature.[7] The monitoring of droplet/particle size during the miniemulsion polymerization process would allow to detect and quantify these changes, thus shedding light on the possible nucleation phenomena that are effective under these conditions.

Spectroscopic techniques such as NIR (near-infrared) and Raman spectroscopy have been shown to be very effective for monitoring different chemical and polymerization processes. In special, in heterogeneous polymerization processes, these techniques can be useful to simultaneous monitoring different variables, such as those related to chemical changes in the reaction medium (e.g., monomer conversion) as well as those related to the physical changes in the particles (e.g., changes in particle size).[8–19] Spectroscopy-based sensors in combination with optical fibers allow the in-line measurements and real-time monitoring of polymerization processes.[18–29]

For the particular case of heterogeneous polymerization reactions, Raman and NIR spectra show two distinct regions, as identified in Figure 1, where different characteristics can be explored: (a) the spectral region that permits to identify chemical information related to the vibrations of the main bonds present in the components (monomer and polymer) and (b) the spectral region with physical information, where the spectrum baseline variation is related to physical properties, such as particle diameter in this case.

In this work, the monitoring of miniemulsion polymerization of styrene is studied using NIR and Raman spectroscopy. Runs with different initial concentrations of surfactant were performed. Monomer conversion and average particle size are measured off-line by reference techniques (gravimetry and dynamic light scattering, respectively) and NIR and Raman spectroscopic techniques were employed for the monitoring of these variables.

2. Experimental Section

Miniemulsion of styrene in water was prepared using a rotor-stator system (T25 Ultra Turrax equipped with a S25N-25G disperser element), which provides high shear rate to produce small monomer droplets, around 300 nm in diameter. Sodium lauryl sulfate (SLS, Vetec, purity > 90 wt%) was employed as a surfactant, hexadecane (HD, Sigma-Aldrich, purity > 99 wt%) and expanded polystyrene (PE) as costabilizers, potassium persulfate initiator (KPS, Synth, > 99 wt%), sodium bicarbonate (Synth, >99.7%) as a buffering agent, and styrene (Innova, > 99.7 wt%) as monomer, as shown in Table 1. All reactants were used as received without further purification.

The prepared miniemulsion was added to a glass reactor (volume 250 mL), under magnetic stirring (700 rpm), heated up to 70 °C and then the water-soluble initiator (potassium persulfate) was added to the reactor. This instant was considered to be the time zero for the polymerization.

The monomer conversion and particle size were monitored in-line using NIR spectroscopy, with a transflectance probe immersed in the medium. Samples were periodically taken from the reactor for the off-line measurements of Raman spectroscopy (IFS 28/N-FT-Raman FRA106, Bruker), gravimetric analysis for determination of conversion and dynamic light scattering (N4 Plus, Coulter Beckman) for determination of average particle size.

2.1. NIR Spectroscopy

The spectral data obtained by NIR spectroscopy were used to infer both monomer conversion and average particle size by setting specific calibration models based on partial least squares (PLS) analysis.[30,31] The calibration was based on the off-line data of conversion (measured by gravimetry) and average particle size (measured by dynamic light scattering, DLS).

For each variable considered, the data are split in two sets. The first set was used to fit the PLS calibration model, and the second one was used to test the model with a data set not used in the calibration (external validation). During the calibration, cross validation methodology (internal validation) was employed to establish the best number of latent variables of the calibration model.[32,33]

2.2. Raman Spectroscopy

Similarly, the spectral data obtained by Raman spectroscopy were also used to infer monomer conversion and average particle size, by employing multivariable linear calibration models based on PLS.

In addition, the data obtained by Raman spectroscopy were used to infer directly the monomer conversion without calibration. The data could be extracted from the spectrum by identifying a characteristic peak that was directly related to the reaction course and a characteristic reference peak of a chemical group or chemical bond that did not change with the reaction. During the batch styrene polymerization, the monomer double bonds (C=C) were consumed, while the amount of aromatic ring remained constant. The Raman spectrum showed a characteristic peak at 1631 cm^{-1}, related to the double bonds, that presented a decreasing area along the polymerization process due to the double bond breaking. The C–H aromatic bond present in both styrene monomer and polystyrene did not change along the reaction and could be used as an internal reference peak to normalize the data, thus filtering the noise fluctuations of the collected spectra.[8,32] The normalized area was calculated using the ratio between the area of the double bond peak (at 1631 cm^{-1}) and the area of the aromatic C–H bond peak (at 1002 cm^{-1}), as indicated in Equation 1

$$\text{Area}_{\text{normalized}} = \frac{\text{Area}_{\text{C=C}}}{\text{Area}_{\text{C–H}}} = \frac{\text{area under the Raman peak at 1631 cm}^{-1}}{\text{area under the Raman peak at 1002 cm}^{-1}} \quad (1)$$

This procedure was performed for each sample time and then the conversion at a given time was calculated by comparing the

Table 1. Experimental formulations.

Components	Function	Mini_1 [g]	Mini_2 [g]	Mini_3 [g]	Mini_4 [g]	Mini_5 [g]
Water	Continuous phase	158.3	153.0	159.1	163.5	158.1
Sodium lauryl sulfate	Surfactant	0.86	0.71	0.70	0.57	0.28
Styrene	Monomer	36.41	35.56	36.22	36.23	36.59
Hexadecane	Costabilizer	1.50	1.41	1.40	1.40	1.41
Polystyrene	Costabilizer	–	0.36	0.44	–	–
Potassium persulfate	Initiator	0.13	0.11	0.11	0.12	0.17
Sodium bicarbonate	Buffer agent	0.03	0.02	0.03	0.03	0.03

normalized area at this specific instant (t) with that at the initial time ($t = 0$), as indicated in Equation 2

$$X_{\text{Raman}}(t) = \text{conversion (at time } t) = 1 - \frac{\text{Area}_{\text{normalized}}(t)}{\text{Area}_{\text{normalized}}(t=0)} \quad (2)$$

The above procedure that does not require PLS calibration was called Raman Direct method.

The other option was the Raman Indirect method, which was analogous to that above described for NIR spectroscopy. In this case, the off line measurements were used to adjust a PLS multilinear calibration model.

2.3. Stability of the Initial Monomer Miniemulsions

The stability of the monomer miniemulsions were evaluated on Samples 6–11, which were prepared with the same formulation as Mini 01 described on Table 1 but with no initiator added. The differences between these samples were the preparation conditions. They were planned according to an experimental design where stirring rate in the high-shear rotor-stator device (from 12000 to 17000 rpm) and time (from 10 to 20 min) were varied to produce monomer miniemulsions with different average droplet sizes.

The stability of the prepared monomer miniemulsions were also evaluated by monitoring, during 2 h, the particle size by dynamic light scattering. Also the light back-scattering patterns of the monomer miniemulsions were evaluated by a Turbiscan equipment (Turbican Lab from Smart Scientific Analysis company).

3. Results and Discussion

3.1. Conversion Results

The results presented in Figure 2 show that, in general, the polymerization was very fast in the first hour of the reaction; after this fast increase, the conversion tends to stabilize after about 2 h. Run Mini_1 presented the highest conversion and fastest polymerization rate, closely followed by Mini_2, Mini_3 and Mini_4. Only the run Mini_5, performed with lower surfactant concentration, presented lower polymerization rate.

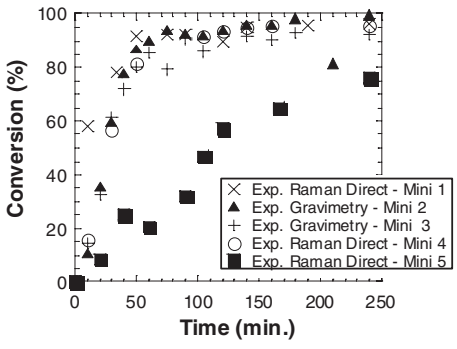

Figure 2. Evolution of conversion in the different runs.

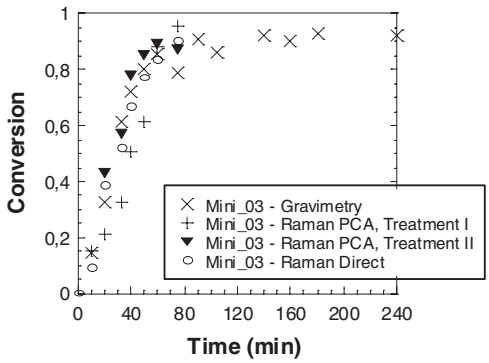

Figure 3. Conversion during run Mini_03 obtained by different methods.

Figure 3 shows the monomer conversion for Mini_3 obtained by the Raman Indirect Method (with two different spectral pretreatments I and II), Raman Direct Method without calibration (Equations 1 and 2 using the selected peak areas) and using gravimetric data (reference). Spectral pretreatment I used the first derivative and pretreatment II used the second derivative, as presented in Table 2. Treatment II fitted best the reference data. The results show a good agreement between the Raman Direct method and the gravimetric data, thus confirming that this method is adequate for conversion monitoring.

The monomer conversion was also determined in-line by NIR spectroscopy, using calibration and internal cross-validation. The runs Mini_02 and Mini_04 were chosen to adjust the model because they have the minimum and maximum values for the conversion (although Mini_05 has the minimum conversion, this reaction was not used as reference because these data presented large oscillations). Therefore, the calibration model can represent a wider range of data. Before the model calibration, some spectral ranges were tested and selected those corresponding to the decrease of the monomer concentration.

The best internal cross-validation result in terms of coefficient of determination (R^2) was 0.96 and root-mean-square error of estimation (RMSEE) was obtained for the first overtone spectral region (5700 to 6200 cm^{-1}) with four principal components. The external validation R^2 was 0.84 and the root-mean-square error of cross validation (RMSECV) was 0.11. Figure 4 shows the external validation of the NIR calibration model for Mini 01 and Mini 03.

3.2. Diameter Results

The experimental data presented in Figure 5 show a strong decrease of the average particle diameter along the first 20 min of the reaction time; then, the particle diameter remained almost constant until the end of the reaction.

Table 2. Pretreatments used for Raman model calibration of conversion.

Identification	Model calibration	Pretreatment	Spectral range Raman shift [cm^{-1}]
Treatment I	Conversion	First derivative + smoothing (Sativsky-Golay filter)	150–400
Treatment II	Conversion	Second derivative	150–400

This period of fast diameter decrease in Figure 5 corresponds to the period of fast conversion increase in Figure 2.

The large surface area (due to the small droplet size) results in most of the surfactant being adsorbed by the monomer droplets. The decrease in particle diameter suggests the coexistence of another nucleation mechanism together with the predominant droplet nucleation, despite the use of surfactant concentration below its nominal critical micellar concentration. Under this condition, little free surfactant is supposed to be still available either to form micelles or to stabilize the polymer formed in the aqueous phase (homogeneous nucleation). The possible mechanisms coexisting with the droplet nucleation are micellar nucleation, homogeneous nucleation and, maybe, some limited emulsion destabilization.[34]

Figure 5 shows the average particle size diameter during run Mini_3 measured using DLS. This measurement represents the diameter used as a reference for the samples analyzed (Mini_01 to Mini_05). Mini_01 shows the smallest diameter because it uses the highest surfactant concentration as indicated in Table 1. For miniemulsion and conventional emulsion polymerization, the particle diameter is inversely proportional to the surfactant concentration; the more surfactant, the smaller the particle diameter.

Figure 6 shows the calculated diameter obtained by Raman spectra and the PCA calibration model, with internal crossvalidation and external validation. This figure compares four different pretreatments used to obtain the best-fit model for the reference data. The different pretreatments and spectral range used are presented in Table 3. These pretreatments are based on first or second derivatives of the spectra and spectral smoothing. When compared with the dynamic light scattering reference data, the best fit was obtained with the pretreatments V and IV that used the full range (0–4000 cm^{-1}) of the Raman spectra.

The model calibration to correlate the particle size with the NIR spectra was based on the data of two experiments, Mini_1 and Mini_5. These experiments were selected to cover a wide range of diameters (100–850 nm). Two different spectral ranges were evaluated and the final calibration model was based on the spectral range 7590–11 700 cm^{-1}. It is important to emphasize that no spectrum pretreatments were used in the NIR calibration model for particle size. This resulted in an internal validation with 2.35 for RMSEE and 0.99 for R^2 and an external

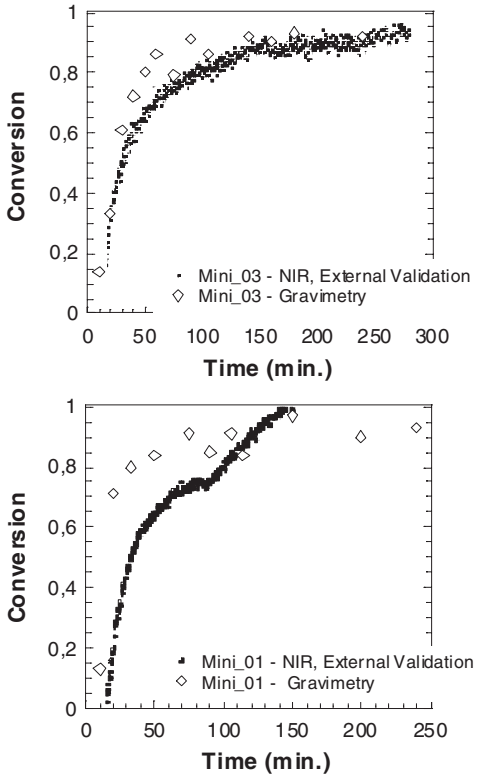

Figure 4. External validation of the NIR calibration model and comparison with gravimetric conversion for runs Mini 01 and Mini 03.

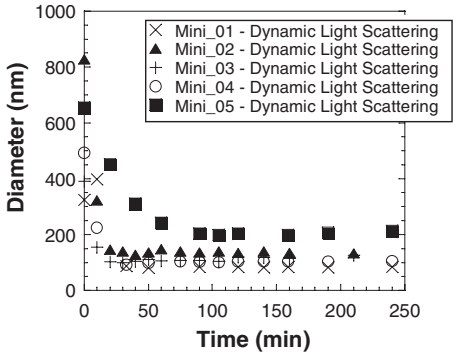

Figure 5. Average particle size measured off-line by dynamic light scattering, for different runs.

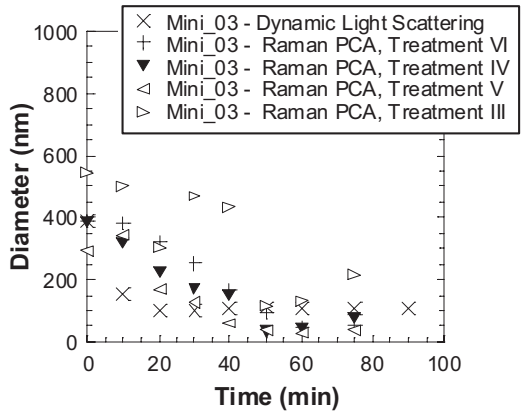

Figure 6. Average particle size obtained by off-line monitoring using Raman Spectroscopy and principal component analysis. Effect of different spectral pre-treatment and comparison with reference measurements with DLS.

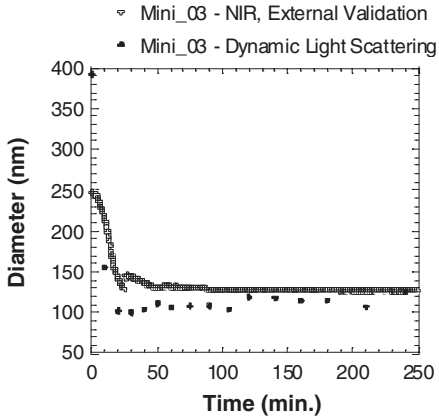

Figure 7. Average particle size: comparison between reference measurements by dynamic light scattering with monitoring using NIR Spectroscopy calibration model during run Mini_03 of miniemulsion polymerization of styrene (external validation, data not used in the calibration model).

validation with 28.4 for RMSECV and 0.86 for R^2, for a model with six principal components.

The comparison between the values of particle size measured off-line by DLS and those monitored in-line by NIR and the respective calibration model, for run Mini_03 not used in the calibration step (external validation) is presented in Figure 7. The NIR model estimations agreed satisfactorily with Dp data determined by DLS. The in-line monitoring by NIR spectroscopy correctly demonstrated the timing of the strong initial decrease of particle size observed for the Mini_03 reaction at around 40 min. The timing of this change in particle size also agrees with the sharp increase in reaction rate (see Figure 2). This result indicates that another particle nucleation mechanism, besides the desired droplet nucleation, took place.

3.3. Comparison between In-Line and Off-Line Methods

Most of the methods here employed to monitor the polymerization reactions were effective and able to satisfactorily estimate the monomer conversion and particle diameter trends. Figure 8 compares the monitored conversion for Mini_03 measured by the Raman direct method and by NIR spectroscopy with the reference gravimetric data.[35] Figure 9 compares the particle size measure for Mini_03 using the Raman method, NIR spectroscopy and the reference dynamic light scattering.

Particle diameter and monomer conversion were effectively monitored and the main trend of these variables was satisfactorily followed; however, for longer reaction times, the particle diameter estimated by the Raman indirect method did not agree well with the reference data measured by DLS. Moreover, there were not enough experimental data to finally validate this lack of fit.

3.4. Stability Results

Figure 5 shows a large variation of particle size along the reaction time, in special during the first period of reaction that corresponds to the main course of the polymerization process. All the experiments of this study were prepared using a high shear rate rotor-stator device to produce small monomer droplets, use of co-stabilizer, and use of surfactant below its nominal critical micellar concentration. Therefore, under these conditions, droplet nucleation would be the only mechanism for production of polymer particles, thus the particle size would be expected

Table 3. Pretreatments used for Raman model calibration of particle size.

Identification	Model calibration	Pretreatment	Spectral range Raman shift [cm^{-1}]
Treatment III	Diameter	First derivative + smoothing (Sativsky-Golay filter)	150–400
Treatment IV	Diameter	Second derivative	150–400
Treatment V	Diameter	Second derivative	0–4000
Treatment VI	Diameter	First derivative + smoothing (Sativsky-Golay filter)	0–4000

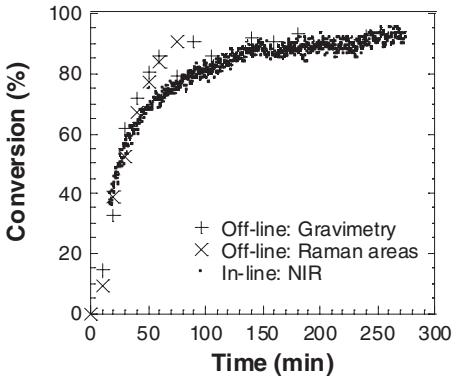

Figure 8. Comparison of conversion measured by gravimetry, by Raman direct method (without calibration) and by NIR spectra and calibration model, for run Mini_03 (miniemulsion polymerization of styrene).

to remain stable and constant along the reaction time, and equal to the initial droplet diameter. However, this behavior was not observed; instead, a strong decrease in particle size was observed in all polymerization runs. In order to understand and to analyze the real cause of the particle size variation, the following probable hypotheses were (i) instability of the initial monomer droplets of the miniemulsion, (ii) occurrence of homogeneous nucleation, and (iii) occurrence of micellar nucleation. The stability of the monomeric miniemulsion was experimentally verified by additional stability tests performed after the miniemulsion preparation and before the polymerization process. DLS (using Coulter equipment) and Multiple Light Scattering (MLS, using Turbiscan equipment) were employed for monitoring the monomeric miniemulsion stability during 2 h after the homogenization process. Figure 10 presents the results for the average droplet size, measured by DLS, of the miniemulsions; no important particle size variation occurred along the evaluation period of 2 h. Figures 11–13 present the results of the changes in

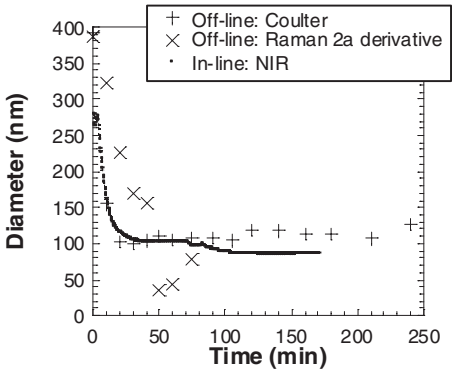

Figure 9. Comparison of particle size measured by dynamic light scattering (Coulter), by Raman spectra and calibration model, and by NIR spectra and calibration model, for run Mini_03 (miniemulsion polymerization of styrene).

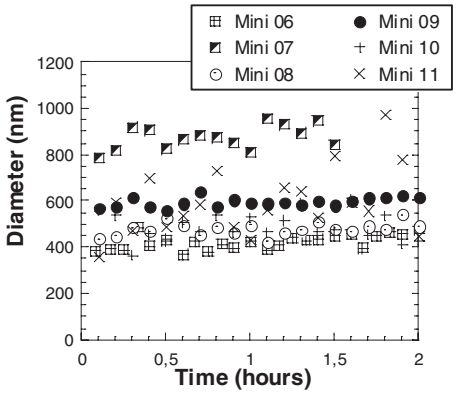

Figure 10. Average droplet size along time after the homogenization process and before the start of the miniemulsion polymerization.

the vertical profile of the back scattered light (MLS) measured in Turbiscan equipment; again no significant delta backscattering variations were observed, confirming that the monomer miniemulsion remained stable along these 2 h of observation. Therefore, the hypothesis (i) can be disregarded.

The measurements of particle size distribution (see Figures 12 and 13) revealed that the average particle size of the polymer particles were about 10-fold (i.e., one order of magnitude) smaller than those of the corresponding average size of the initial monomer droplets. The particle size distribution was measured by DLS at the beginning of the reaction and after a time range. Each sample was analyzed in duplicate (indices 1/2, 2/2 were used), triplicate (indices 1/3, 2/3, and 3/3 were used) or quadruplicate (indices 1/4, 2/4, ¾, and 4/4 were used) and only one sample had just a single measurement (index 1/1 was used). This strong shift of the distribution toward smaller particles is evidence that the nucleation of smaller particles occurred. This can be attributed to either micellar or homogeneous nucleation. Our experiments were carried out using low emulsifier concentrations (from 15 to 5 mmol L^{-1}) that are in the range of critical micelle concentration (CMC) of sodium lauryl sulfate (7 mmol L^{-1}) reported in the literature. A fraction of surfactant is adsorbed by the monomers droplets leading to free surfactant on aqueous phase below CMC, making weak the hypothesis (iii) of micellar nucleation. The remaining hypothesis (ii) is that homogeneous nucleation coexists with droplets nucleation at the beginning of the polymerization process.

The presence of small particles formed by oligomer precipitation due to its low solubility in water (homogenous nucleation) would form only particles up to four monomers because j_{crit} is equal to 5.[36] The oligomer size was considered to have the same diameter as a micelle. For the case studied, the surfactant used was sodium lauryl sulfate, whose micelle characteristic radius is

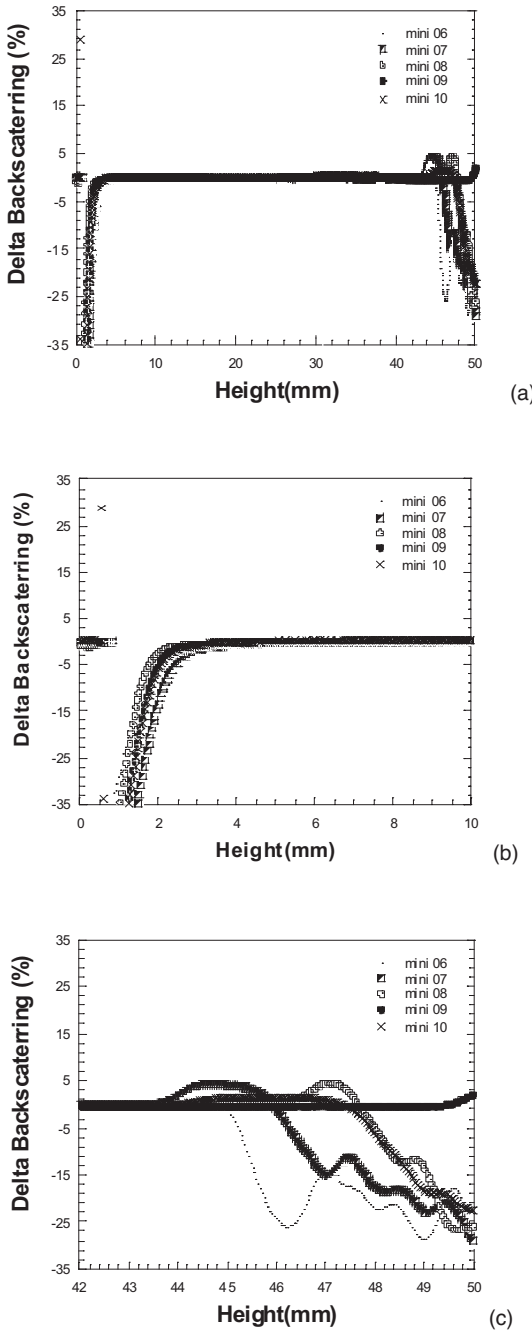

Figure 11. Samples of delta backscattering after 2 h of homogenization process and before the start of the miniemulsion polymerization: a) full profile; b) amplification of the region 0–10 mm; c) amplification of the region 42–50 mm.

2.6 nm.[37] However, the particles would have diameters of about 1 nm. Hence, considering that the hypothesis of homogeneous nucleation is true, the initial particle size distribution of Mini_02 in Figure 12 and of Mini_03 in Figure 13 should present particle diameter reduction when compared with the final particle size. Observing

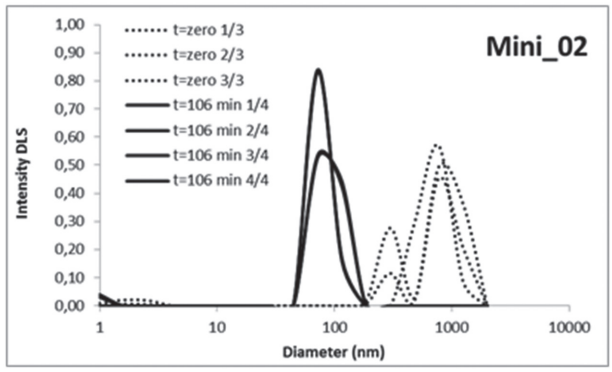

Figure 12. Particle diameter distribution for Mini_02.

Figures 12 and 13, we can identify particles with size of 1 nm at the beginning of the process, demonstrating the existence of nucleation of smaller particles. However, this range is almost out the reliable range of analytical instrument used. So, unfortunately, the measurements in Figures 12 and 13 are not enough to clear distinguish between homogenous and micellar nucleation, so we cannot be conclusive on what is the mechanism of nucleation of smaller particles that is operative under these conditions. More specific experiments should be devised in future efforts to clarify these phenomena.

4. Conclusions

The aim of this work was to evaluate monomer conversion and particle diameter using off-line Raman spectroscopy and in-line NIR spectroscopy monitoring. The methodologies analyzed presented suitable results and were reasonably well fit to the experimental data measured by reference methods.

This study validated the methods proposed for monitoring conversion and also compared the methodologies evaluated, identifying NIR spectroscopy as an effective method for real-time, in-line, in-situ monitoring simultaneously monomer conversion and particle size, not

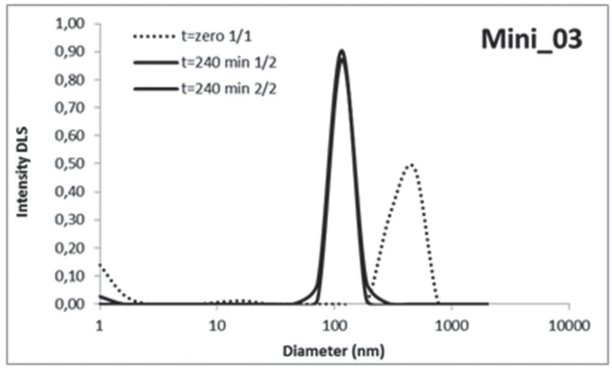

Figure 13. Particle diameter distribution for Mini_03.

requiring sample preparation, supplying information with no time delay and at shorter intervals, preventing the loss of process information.

Moreover, exploiting the experimental results, an attempt to explain the strong reduction of the polymer particle size vis-à-vis the initial monomer droplet size observed during the miniemulsion polymerization, three potential hypotheses were analyzed: (i) instability of the miniemulsion monomer droplets, (ii) homogeneous nucleation, and (iii) micellar nucleation. The results showed that homogenous nucleation and micellar nucleation can possibly co-exist with the droplets nucleation at the beginning of the reaction time. In-line, real-time measurements are of fundamental importance to follow the rapid changes that take place in the process.

It is shown that the use of the spectroscopic monitoring techniques allows the real-time measurements of these variables, which can be insightful to see quick changes that, otherwise, would be difficult to identify by more infrequent sampling and off-line measurements. In particular, we observe significant changes in size from the initial droplets to the final polymer particles, an indication that nucleation mechanisms other from the classical droplet nucleation may take place.

Acknowledgements: The authors thank CAPES (grant number 01/2007-Procad), CNPq (grant numbers 304321/2011-7 and 480463/2004-2), and FAPESP (grant number 13/50218-2) for the financial support, and Prof. Frank Quina for revising the manuscript.

Received: February 28, 2016; Revised: May 8, 2016; Published online: June 29, 2016; DOI: 10.1002/mren.201600013

Keywords: miniemulsion polymerization; NIR spectroscopy; on-line monitoring; Raman spectroscopy

[1] C. S. Chern, *Prog. Polym. Sci.* **2006**, *31*, 443.
[2] F. J. Schork, Y. Luo, W. Smulders, J. P. Russum, A. Butté, K. Fontenot, *Adv. Polym. Sci.* **2005**, *175*, 129.
[3] J. M. Asua, in *Polymer Reaction Engineering* (Ed: J. M. Asua), Blackwell, Oxford, UK **2007**.
[4] J. M. Asua, *Prog. Polym. Sci.* **2002**, *27*, 1283.
[5] F. J. U. Schork, G. W. Poehlein, S. Wang, J. Reimers, J. Rodrigues, *Colloids Surf., A* **1999**, *153*, 39.
[6] V. Mittal, in *Miniemulsion Polymerization Technology* (Ed: V. Mittal), John Wiley & Sons, Inc., Hoboken, NJ, USA **2010**.
[7] L. I. Ronco, R. J. Minari, L. M. Gugliotta, *Braz. J. Chem. Eng.* **2015**, *32*, 191.
[8] M. M. Reis, P. H. H. Araújo, C. Sayer, R. Giudici, *J. Appl. Polym. Sci.* **2004**, *93*, 1136.
[9] M. M. Reis, P. H. H. Araújo, C. Sayer, R. Giudici, *Polymer* **2003**, *44*, 6123.
[10] M. M. Reis, P. H. H. Araújo, C. Sayer, R. Giudici, *Macromol. Rapid Commun.* **2003**, *24*, 620.
[11] M. M. Reis, P. H. Araujo, C. Sayer, R. Giudici, *Macromol. Symp.* **2004**, *206*, 165.
[12] M. M. E. Colmán, *PhD Thesis*, Universidade Federal de Santa Catarina **2013**.
[13] J. C. Santos, C. N. Lopes, M. M. Reis, R. Giudici, C. Sayer, R. A. F. Machado, P. H. H. Araújo, *Braz. J. Chem. Eng.* **2008**, *25*, 399.
[14] M. K. Lenzi, E. L. Lima, J. C. Pinto, *J. Near Infrared Spectrosc.* **2006**, *14*, 179.
[15] M. M. Reis, M. Uliana, C. Sayer, P. H. H. Araújo, R. Giudici, *Braz. J. Chem. Eng.* **2005**, *22*, 61.
[16] M. M. Reis, P. H. H. Araujo, C. Sayer, R. Giudici, *Anal. Chim. Acta.* **2007**, *595*, 257.
[17] J. G. F. Santos, D. V. Way, P. A. Melo, M. Nele, J. C. Pinto, *Macromol. Symp.* **2011**, *299*, 57.
[18] G. E. Fonseca, M. A. Dubé, A. Penlidis, *Macromol. React. Eng.* **2009**, *3*, 327.
[19] A. F. Santos, F. M. Silva, M. K. Lenzi, J. C. Pinto, *Polym.-Plast. Technol. Eng.* **2005**, *44*, 1.
[20] R. Giudici, *Lat. Am. Appl. Res.* **2000**, *30*, 351.
[21] D. C. H. Chien, A. Penlidis, *J. Macromol. Sci., Rev. Macromol. Chem. Phys.* **1990**, *30*, 1.
[22] O. Kammona, E. G. Chatzi, C. Kiparissides, *J. Macromol. Sci., Rev. Macromol. Chem. Phys.* **1999**, *C39*, 57.
[23] W. D. Hergeth, *Ullmann's Encyclopedia of Industrial Chemistry*, Wiley-VCH, Weinheim, Germany **2001**.
[24] M. van den Brink, M. Pepers, A. M. van Herk, *J. Raman Spectrosc.* **2002**, *33*, 264.
[25] A. M. Cardenas-Valencia, V. Shastry, L. H. Garcia-Rubio, *In Situ Spectroscopy of Monomer and Polymer Synthesis*, pp. 83–108, Springer, US **2003**.
[26] J. R. Richards, J. P. Congalidis, *Comput. Chem. Eng.* **2006**, *30*, 1447.
[27] W. K. Silva, D. L. Chicoma, R. Giudici, *Polym. Eng. Sci.* **2011**, *51*, 2024.
[28] E. Frauendorfer, A. Wolf, W. D. Hergeth, *Chem. Eng. Technol.* **2010**, *33*, 1767.
[29] A. F. Santos, F. M. Silva, M. K. Lenzi, J. C. Pinto, in *Monitoring Polymerization Reactions: From Fundamentals to Applications* (Eds: W. F. Reed, A. M. Alb), John Wiley & Sons, Hoboken **2013**, Ch. 6, p. 107.
[30] C. Pasquini, *J. Braz. Chem. Soc.* **2003**, *14*, 198.
[31] M. M. Reis, P. H. Araújo, C. Sayer, R. Giudici, *Ind. Eng. Chem. Res.* **2004**, *43*, 7243.
[32] J. C. Santos, M. M. Reis, R. A. Machado, A. Bolzan, C. Sayer, R. Giudici, P. H. Araújo, *Ind. Eng. Chem. Res.* **2004**, *43*, 7282.
[33] D. L. Chicoma, C. Sayer, R. Giudici, *Macromol. React. Eng.* **2001**, *5*, 150.
[34] K. Landfester, F. J. Schork, V. A. Kusuma, *C. R. Chim.* **2003**, *6*, 1337.
[35] P. M. N. Ambrogi, *PhD Thesis*, Universidade de São Paulo **2015**.
[36] M. J. Ballard, R. G. Gilbert, D. H. Napper, P. J. Pomery, P. W. O'Sullivan, J. H. O'Donnell, *Macromolecules* **1986**, *19*, 1303.
[37] E. M. Coen, R. G. Gilbert, B. R. Morrison, H. Leube, S. Peach, *Polymer* **2006**, *39*, 7099.